Cellular and Molecular Bioengineering (2023) 16:127–141
https://doi.org/10.1007/s12195-023-00762-2

BMES BIOMEDICAL ENGINEERING SOCIETY

ORIGINAL ARTICLE

Angiotensin II Increases Oxidative Stress and Inflammation in Female, But Not Male, Endothelial Cells

Callie M. Weber[1] · Mikayla N. Harris[2] · Sophia M. Zic[1] · Gurneet S. Sangha[1] · Nicole S. Arnold[2] · Douglas F. Dluzen[2] · Alisa Morss Clyne[1]

Received: 19 October 2022 / Accepted: 29 March 2023 / Published online: 12 April 2023
© The Author(s) under exclusive licence to Biomedical Engineering Society 2023

Abstract

Introduction Women are at elevated risk for certain cardiovascular diseases, including pulmonary arterial hypertension, Alzheimer's disease, and vascular complications of diabetes. Angiotensin II (AngII), a circulating stress hormone, is elevated in cardiovascular disease; however, our knowledge of sex differences in the vascular effects of AngII are limited. We therefore analyzed sex differences in human endothelial cell response to AngII treatment.

Methods Male and female endothelial cells were treated with AngII for 24 h and analyzed by RNA sequencing. We then used endothelial and mesenchymal markers, inflammation assays, and oxidative stress indicators to measure female and male endothelial cell functional changes in response to AngII.

Results Our data show that female and male endothelial cells are transcriptomically distinct. Female endothelial cells treated with AngII had widespread gene expression changes related to inflammatory and oxidative stress pathways, while male endothelial cells had few gene expression changes. While both female and male endothelial cells maintained their endothelial phenotype with AngII treatment, female endothelial cells showed increased release of the inflammatory cytokine interleukin-6 and increased white blood cell adhesion following AngII treatment concurrent with a second inflammatory cytokine. Additionally, female endothelial cells had elevated reactive oxygen species production compared to male endothelial cells after AngII treatment, which may be partially due to nicotinamide adenine dinucleotide phosphate oxidase-2 (NOX2) escape from X-chromosome inactivation.

Conclusions These data suggest that endothelial cells have sexually dimorphic responses to AngII, which could contribute to increased prevalence of some cardiovascular diseases in women.

Keywords Sex differences · Vasculature · IL-6 · Reactive oxygen species

Abbreviations

SORCS2	Sortilin related VPS10 domain containing receptor 2
CCR7	Chemokine (C–C motif) receptor 7
TPM3P7	Tropomycin 3 psuedogene 7
SIM1	Single-minded homolog 1
IL-6	Interleukin-6
TGF-β2	Transforming growth factor beta 2
LSS	Lanosterol synthase
DHX16	DEAH-box helicase 16
WASH8P	WAS protein family homolog 8, pseudogene
CDNF	Cerebral dopamine neurotrophic factor
GTF2H2	General transcription factor IIH subunit II
RRN3	RNA polymerase I transcription factor
GBA	Glucosylceramidase beta 1
NDUFC2	NADH:Ubiquinone oxidoreductase subunit C2
NDUFA1	NADH:Ubiquinone oxidoreductase subunit A1
UQCR10	Ubiquinol-cytochrome C reductase, complex III, subunit X
UQCRQ	Ubiquinol-cytochrome C reductase, complex III, subunit VII

Associate Editor Michael R. King oversaw the review of this article.

✉ Alisa Morss Clyne
aclyne@umd.edu

[1] Fischell Department of Bioengineering, University of Maryland, 8278 Paint Branch Dr., College Park, MD 20742, USA

[2] Department of Biology, Morgan State University, Baltimore, MD 21251, USA

COX6A1	Cytochrome C oxidase subunit 6A1
COX7C	Cytochrome C oxidase subunit 7C
COX17	Cytochrome C oxidase copper chaperone
ATP5F1E	ATP synthase F1 subunit epsilon
ATP5ME	ATP synthase membrane subunit E
CYBB	Cytochrome B-245 beta chain
NOX2	NADPH oxidase 2
αSMA	Alpha smooth muscle actin
TNFα	Tumor necrosis factor alpha
ARID5A	AT-Rich interaction domain 5A
ZC3H12A	Reagenase-1

Introduction

Cardiovascular disease, which initiates with endothelial cell (EC) dysfunction, is the leading cause of death in both men and women [1]. While women are largely protected against ischemic heart disease prior to menopause, the benefits afforded to women are diminished after menopause. Furthermore, some vascular diseases are more common in women than in men. Women are 1.8 times more likely to be diagnosed with pulmonary arterial hypertension (PAH) than men [2], nearly two-thirds of Americans with Alzheimer's disease are women [3], and women with diabetes have myocardial infarctions earlier and with greater mortality than men with diabetes [4]. To develop sex- and gender-specific cardiovascular care, it is essential to understand sex differences in cardiovascular disease.

While studies of cardiovascular disease sex differences historically focused on sex hormones, recent transcriptomic studies suggest that 14–25% of the EC transcriptome is sex-dependent [5]. These EC sex differences may be a product of increased X-linked gene expression through escape from X-chromosome inactivation (XCI). Approximately 15% of X-linked genes consistently escape XCI, and an additional 10% of X-linked genes show variable inactivation patterns [6]. XCI escape of genes such as *CYBB* [7], which codes for NADPH oxidase-2 (NOX2), could increase oxidative stress in female cells, contributing to EC dysfunction.

Transcriptomic differences in female and male EC may be best studied in human umbilical vein endothelial cells (HUVEC), which exhibit the sex of the newborn [8–10] and have not been exposed to sex hormones in vivo. Indeed, in hormone-naive HUVEC from boy-girl twin pairs, there were more than 2000 differentially expressed genes [5]. Female HUVEC further increased endothelial nitric oxide synthase (eNOS) expression and intracellular ATP, were more proliferative and migratory, and decreased mitochondrial respiration following VEGF-stimulation compared to male HUVEC [9, 10]. A recent study further showed that female and male HUVEC have different responses to mechanical cues such as shear stress and substrate stiffness [11]. Thus, female and male HUVEC may have different transcriptomes at baseline and in response to external stimuli.

Angiotensin II (AngII) is a circulating stress hormone [12] that contributes to endothelial dysfunction in vascular disease. When AngII binds to the angiotensin type 1 receptor (AT1R), it enhances NOX2 activity to increase reactive oxygen species (ROS) production [13], leading to EC dysfunction. AngII is elevated in hypertension [14] and is commonly infused in rodents to induce hypertension [15]. Interestingly, AngII has also been implicated in vascular diseases that are more prevalent in women, such as PAH and Alzheimer's disease.

Most studies on the effects of AngII on vascular and EC function have only been conducted in male rodents [16–19] or failed to analyze outcomes in a sex-dependent manner [20]. Therefore, in this study we examined how female and male HUVEC responded differently to AngII. We used RNA sequencing to study transcriptomic differences, followed by phenotypic, inflammatory, and oxidative stress assays to measure how the transcriptomic differences affected EC function. Our data demonstrate that EC have sexually dimorphic oxidative stress and inflammatory responses to AngII treatment, which could be important in treating cardiovascular disease in female versus male patients.

Methods

Cell Culture

Male and female endothelial cells from donors of different sexes and from different vascular beds were used (Table 1), as indicated in each experiment. Pooled male and pooled female human umbilical vein endothelial cells (HUVEC; Lonza; 3 donors per sex), individual donor male and female HUVEC (Lonza, 2 donors per sex), and individual donor male and female human coronary artery endothelial cells (HCAEC; Lifeline Cell Technology; 1 donor per sex) were cultured in Endothelial Growth Medium-2 (EGM-2; Lonza) supplemented with 10% fetal bovine serum (FBS; Hyclone), 1% penicillin streptomycin (Thermo Fisher) and 1% L-glutamine (Thermo Fisher). Individual donor human pulmonary artery endothelial cells (HPAEC; Pulmonary Hypertension Breakthrough Initiative; 3 donors per sex) were cultured in Endothelial Growth Medium-2-MV (EGM-2-MV; Lonza) supplemented with 10% FBS, 1% penicillin streptomycin, and 1% L-glutamine. Cells were maintained in an incubator with 5% CO_2 at 37 °C and used between passages 4–9.

RNA Sequencing

Confluent pooled male and female HUVEC were incubated with 1 μM angiotensin II (AngII; Sigma; SCP0020) or water

Table 1 EC donor characteristics

Source tissue	Cell sex	Donor age	Race
Umbilical vein	Female (3 pooled donors)	Newborn	White
Umbilical vein	Male (3 pooled donors)	Newborn	White
Umbilical vein	Female	Newborn	White
Umbilical vein	Male	Newborn	White
Umbilical vein	Female	Newborn	Black or African American
Umbilical vein	Male	Newborn	Black or African American
Pulmonary artery	Female	36	White
Pulmonary artery	Male	49	White
Pulmonary artery	Female	50	White
Pulmonary artery	Male	51	White
Pulmonary artery	Female	34	White
Pulmonary artery	Male	40	White
Coronary artery	Female	12	Black or African American
Coronary artery	Male	22	Black or African American

as a vehicle control for 24 h. RNA was extracted using phenol/chloroform [21]. Briefly, cells were washed with cold phosphate buffered saline (PBS), scraped, and centrifuged at 17,000×*g* and 4 °C for 4 min. 1 mL TRIzol (ThermoFisher) was added to each sample, after which the cell pellets were resuspended and incubated at room temperature for 5 min. 200 µL chloroform (Sigma) was added to each sample, and samples were vortexed and centrifuged at 4 °C and 17,000×*g* for 30 min. Equal volumes of the top RNA sample layer and isopropyl alcohol were combined with a 1:100 dilution of GlycoBlue Co-precipitant (ThermoFisher) and then centrifuged at 4 °C and 17,000×*g* for 30 min. The pellet was washed with ice-cold 70% ethanol and resuspended in RNase-free water. RNA was quantified on a Nanodrop 2000c (Thermo Fisher) and then shipped to Novogene where ribosomal RNA were degraded and a directional RNA library was constructed to extract long non-coding RNA, micro RNA, and circular RNA before the samples were sequenced on an Illumina NovaSeq 6000.

All RNAseq data were processed in Galaxy (https://usegalaxy.org). A FASTQC report was used to verify RNA sequencing quality. Samples were trimmed as paired end reads using Trimmomatic and aligned to the human genome (hg38) using HISAT2. FeatureCounts measured differentially expressed genes (DEG) based on the annotated human genome. EdgeR was then used to compare AngII treated samples to untreated samples for both the male and female HUVEC. A Benjamini and Hochberg p-value adjustment was used for statistical analysis. Genes with a fold change > 0.6 and an adjusted p-value < 0.3 were considered statistically significant. The EdgeR report was uploaded to iPathway Guide [22, 23] (Advaita Bio) to visualize gene and pathway alterations in response to AngII, and how DEG differed between male and female HUVEC following AngII treatment.

ELISA

Human interleukin-6 (IL-6) and transforming growth factor-β2 (TGF-β2) in cell culture media samples were quantified by ELISA (RayBiotech) as per manufacturer's protocols. For the TGF-β2 ELISA, cells were treated ± 1 µM AngII for 24 h after which 250 µL conditioned media was transferred to microcentrifuge tubes, activated with 50 µL 1N HCl (Sigma) for 10 min, and then neutralized with 50 µL 1.2 N NaOH (Sigma)/ 0.5 M HEPES (Sigma). For the IL-6 ELISA, cells were treated ± 1 µM AngII and ± 1 ng/mL TNFα for 24 h. Conditioned media was diluted 1:1 in sample dilution buffer. Absorbance was read immediately on a plate reader (Tecan Spark Multimode Microplate Reader) at 450 nm.

Endothelial-to-Mesenchymal Transition (EndMT)

Endothelial vs. mesenchymal cell phenotype was measured using an endothelial marker (VE-cadherin) and a mesenchymal marker (α-smooth muscle actin; αSMA). Confluent pooled male and female HUVEC on 18 mm glass coverslips (VWR) were treated ± 1 µM AngII for 24 h, fixed in 4% paraformaldehyde (PFA; Sigma), and then permeabilized and blocked with 0.2% TritonX-100 (Alfa Aesar) and 5% goat serum (Sigma) in phosphate buffered saline (PBS; Thermo Fisher) for 1 h. Cells were incubated in primary antibodies against VE-cadherin (1:50, Santa Cruz Biotechnology; sc-9989) and αSMA (1:200; Abcam; ab5694) overnight at 4 °C in 1% goat serum in PBS. Cells were then incubated in the appropriate secondary antibodies (1:1000; Thermo Fisher) and Hoechst (1:2000; nuclei; Thermo Fisher). Samples were imaged on an ECHO Revolve microscope at 20x magnification.

White Blood Cell (WBC) Adhesion Assay

WBC adhesion was used to determine EC inflammation. Confluent male and female HUVEC and HPAEC were treated ± 1 μM AngII and ± 1 ng/mL TNFα for 24 h. WBC were isolated from freshly drawn blood following IRB 1818450-1 using Acrodisc WBC Syringe Filters (Pall). WBC were labeled with Calcein AM (Thermo Fisher) for 30 min in EGM-2 media, after which they were washed and resuspended at 2×10^6 cells/mL in EGM-2. HUVEC and HPAEC were washed with 1 × PBS, then incubated with 1×10^6 WBC for 10 min. After thorough washing, samples were imaged on an ECHO Revolve microscope at 10x magnification.

Oxygen Consumption Rate (OCR)

EC oxidative phosphorylation was measured using a Seahorse ATP Rate Assay (Agilent). Male and female pooled HUVEC were seeded at 40,000 cells/well in a 96-well Seahorse plate (Agilent), allowed to attach overnight, then treated ± 1 μM AngII for 24 h. The ATP Rate Assay was run following manufacturer's protocols. OCR, an approximation of mitochondrial metabolism, was assessed in basal conditions and following oligomycin (ATP synthase inhibitor) and rotenone/antimycin A (mitochondrial electron transport chain inhibitors) treatment. Mitochondrial ATP production was calculated using Seahorse Wave software (Agilent), and proton leak was calculated as the difference between oligomycin and rotenone/antimycin A inhibition of OCR.

Reactive Oxygen Species

Carboxy-H_2DCFDA, which is taken up by a cell and then oxidized by ROS to induce a fluorescent signal, and MitoSOX, which is targeted to the mitochondria then specifically oxidized by superoxide to produce a fluorescent signal, were used to measure EC oxidative stress. Confluent male and female HUVEC and HPAEC were treated ± 1 μM AngII (Millipore Sigma; SCP0020) for 24 h. Cells were washed twice with Hank's Balanced Salt Solution with calcium and magnesium (HBSS/Ca/Mg; Thermo Fisher) and then incubated in 25 μM carboxy-H_2DCFDA (Thermo Fisher) in HBSS/Ca/Mg containing 1 μM Hoechst for 30 min at 37 °C. HBSS without sodium bicarbonate (Thermo Fisher) was used to wash the cells before mounting them on glass slides and imaging at 10x magnification on an ECHO Revolve microscope. For the MitoSOX assay, HUVEC were washed with HBSS/Ca/Mg and then incubated in HBSS/Ca/Mg containing 5 μM MitoSOX (Thermo Fisher) and 1 μM Hoechst for 15 min at 37 °C. After washing with HBSS without sodium bicarbonate, samples were mounted on glass slides and immediately imaged on an ECHO Revolve fluorescent microscope.

CYBB Gene Expression

HUVEC, HCAEC, and HPAEC were seeded at 125,000 cells/well in a 12-well plate. RNA was isolated from confluent EC using an RNEasy Mini Kit (Qiagen). Isolated RNA was quantified on a Nanodrop 2000c (Thermo Fisher), and RNA was converted to cDNA using a High-Capacity cDNA Reverse Transcription kit (Thermo Fisher) and a ProFlex Thermal Cycler (Thermo Fisher). We ran qPCR using a Taqman probe for *CYBB* (ThermoFisher; Hs00166163_m1) and *RPLP0,* a ribosomal protein not differentially expressed between male and female EC, as a housekeeper (Thermo Fisher; Hs00420895_gH) using a QuantStudio 7 Flex qPCR System (Thermo Fisher).

NOX2 siRNA Knockdown

Pooled HUVEC were seeded at 125,000 cells/well in a 12-well plate in antibiotic-free EGM-2 supplemented with 10% FBS and 1% glutamine. After 24 h, 18 pmol CYBB siRNA (Thermo Fisher; s531913) or Silencer Select Negative Control #1 (Thermo Fisher) complexed with Lipofectamine RNAiMAX Transfection Reagent (Thermo Fisher) in Opti-MEM I Reduced Serum Medium (Thermo Fisher) was added to the culture medium. After 24 h of siRNA treatment, cells were treated with 1 μM AngII, and the downstream assay was performed.

NOX2 protein was assessed by Western blot. 6, 24, or 48 h after *CYBB* siRNA application, cells were lysed. Protein was quantified using a BCA assay (Thermo Fisher), and samples (3.5 μg/μL protein) were separated on 4–12% Bis–Tris gels (Thermo Fisher) and transferred to a nitrocellulose membrane (Thermo Fisher) using an iBlot 2 (Thermo Fisher). Membranes were blocked for 1 h in 5% bovine serum albumin (Millipore Sigma) in PBS containing 0.5% Tween 20 (Thermo Fisher) and then incubated with primary antibodies for NOX2 (Proteintech; 19013-1-AP; 1:1000) and β-Actin (Santa Cruz Biotechnology; sc-47778; 1:1000) overnight. After thorough washing, membranes were incubated in the appropriate secondary antibodies (Promega; 1:2000) for 2 h. Western blots were imaged on an Alpha Innotech Fluorchem Imager (Protein Simple), and proteins were quantified using AlphaView software.

Fluorescent Image Quantification

Fluorescent images were quantified in Fiji (ImageJ). For EndMT analysis, rolling ball background subtract was used to remove background fluorescence. Images were then

thresholded to remove non-specific labeling before measuring fluorescence intensity. Thresholds were maintained for all images in an experiment, and fluorescence intensity was normalized to cell count by dividing by the number of nuclei in the same image. For WBC adhesion analysis, the number of adhered WBC per frame were counted and averaged between samples. Images shown are representative of the average fluorescence intensity for each treatment group.

Statistics

Statistics were analyzed in GraphPad Prism. Non-parametric Mann–Whitney tests, Kruskal–Wallis tests, and two-way ANOVA with a Tukey's correction for multiple comparisons were used to compare datasets. RNA-seq data were considered biologically significant with an adjusted p-value < 0.3 and a $Log_2FC > 0.6$.

Results

AngII is a circulating stress hormone known to have vascular effects. Since the EC transcriptome itself is sexually dimorphic [5], we investigated if AngII has different effects on female versus male EC. We first studied gene expression differences in pooled HUVEC from male and female donors. RNA sequencing showed that male and female HUVEC had 1134 differentially expressed genes. 622 genes were upregulated in female as compared to male HUVEC, and 512 genes were upregulated in male as compared to female HUVEC (Fig. 1A, Table S1A–B). Cell sex was validated through expression of sex-specific transcripts including the female-associated gene X-Inactive Specific Transcript (*XIST),* which was downregulated in male compared to female HUVEC *(*$Log_2FC = 14.16$), and the male-associated gene Ubiquitin specific peptidase 9 Y-Linked (*USP9Y*), which is upregulated in male compared to female HUVEC ($Log_2FC = 14.19$).

We then treated pooled male and female HUVEC with AngII for 24 h and analyzed gene expression changes. Female HUVEC differentially expressed 444 genes with AngII treatment, while male HUVEC differentially expressed 21 genes (Fig. 1B; Table S2A–B). The 172 upregulated genes in female AngII-treated HUVEC included interleukin-6 (*IL-6*; $p = 0.006$), an inflammatory cytokine, and transforming growth factor β-2 (*TGF-β2*; $p < 0.0001$), a growth factor involved in proliferation, differentiation, and apoptosis. The 272 downregulated genes included dual specificity phosphatase 8 (*DUSP8*; $p = 0.008$), a phosphatase regulating protein responsible for cell proliferation and differentiation. The 8 upregulated genes in AngII-treated male HUVEC included glucosylceramidase β (*GBA*; $p < 0.0001$), a lysosomal protein involved in glycolipid metabolism, while the 13 downregulated genes included RNA polymerase I transcription factor (*RRN3*; $p < 0.0001$; Fig. 1C), an RNA polymerase regulating apoptosis and transcription. Of the differentially expressed genes, only lanosterol synthase (*LSS*; $p < 0.0001$), an enzyme involved in cholesterol synthesis, was commonly downregulated.

We next used iPathway Guide's KEGG database to understand how these expression changes relate to cell-level functions. Male HUVEC treated with AngII did not have any KEGG pathways with three or more differentially expressed genes. However, female HUVEC treated with AngII had multiple KEGG pathways with more than three differentially expressed genes. Of particular interest were statistically significant changes in pathways that could be important in AngII-related diseases that are more prevalent in women, including tumor necrosis factor (TNF) signaling, advanced glycation end products (AGE)-receptor for advanced glycation end products (RAGE) signaling, cytokine-cytokine receptor interaction, metabolic pathways, oxidative phosphorylation, and pathways of neurodegeneration (Fig. 1D, Table S3).

To determine if gene expression changes resulted in cell function changes, we further investigated several genes that were upregulated in AngII-treated female HUVEC. TGF-β2 is a major molecular player in EndMT [34], which can contribute to pulmonary hypertension predisposition and disease progression [25]. Since TGF-β2 expression was higher in pooled female, but not significantly altered in male, AngII-treated HUVEC (Fig. 2A), we measured TGF-β2 protein and EndMT in female and male HUVEC. TGF-β2 protein did not change after 24 h of AngII treatment in pooled cells of either sex (Fig. 2B). Similarly, VE-cadherin did not decrease and α-smooth muscle actin (αSMA) did not increase with AngII treatment in either male or female cells, suggesting that AngII did not lead to EndMT (Fig. 2C). Thus, even though AngII increased *TGF-β2* mRNA expression in female HUVEC, this did not lead to measurable changes in TGF-β2 protein or EndMT.

IL-6, an inflammatory cytokine implicated in diseases such as diabetes and Alzheimer's disease, expression levels were also higher in pooled female HUVEC but unchanged in male HUVEC following AngII treatment (Fig. 3A). Adhesion protein genes, including E-Selectin (*SELE;* $Log_2FC = 0.601$), vascular cell adhesion protein-1 (*VCAM1;* $Log_2FC = 0.455$), and intercellular adhesion molecule-1 (*ICAM1;* $Log_2FC = 0.399$) were elevated in pooled female, but not male, HUVEC following AngII treatment. IL-6 protein released into the media did not change between cells of differing sex or with AngII treatment (Fig. 3B, C). Based on these results, we hypothesized that a second inflammatory stimulus may be needed to change IL-6 release. We therefore treated pooled male and female HUVEC with both AngII and the inflammatory

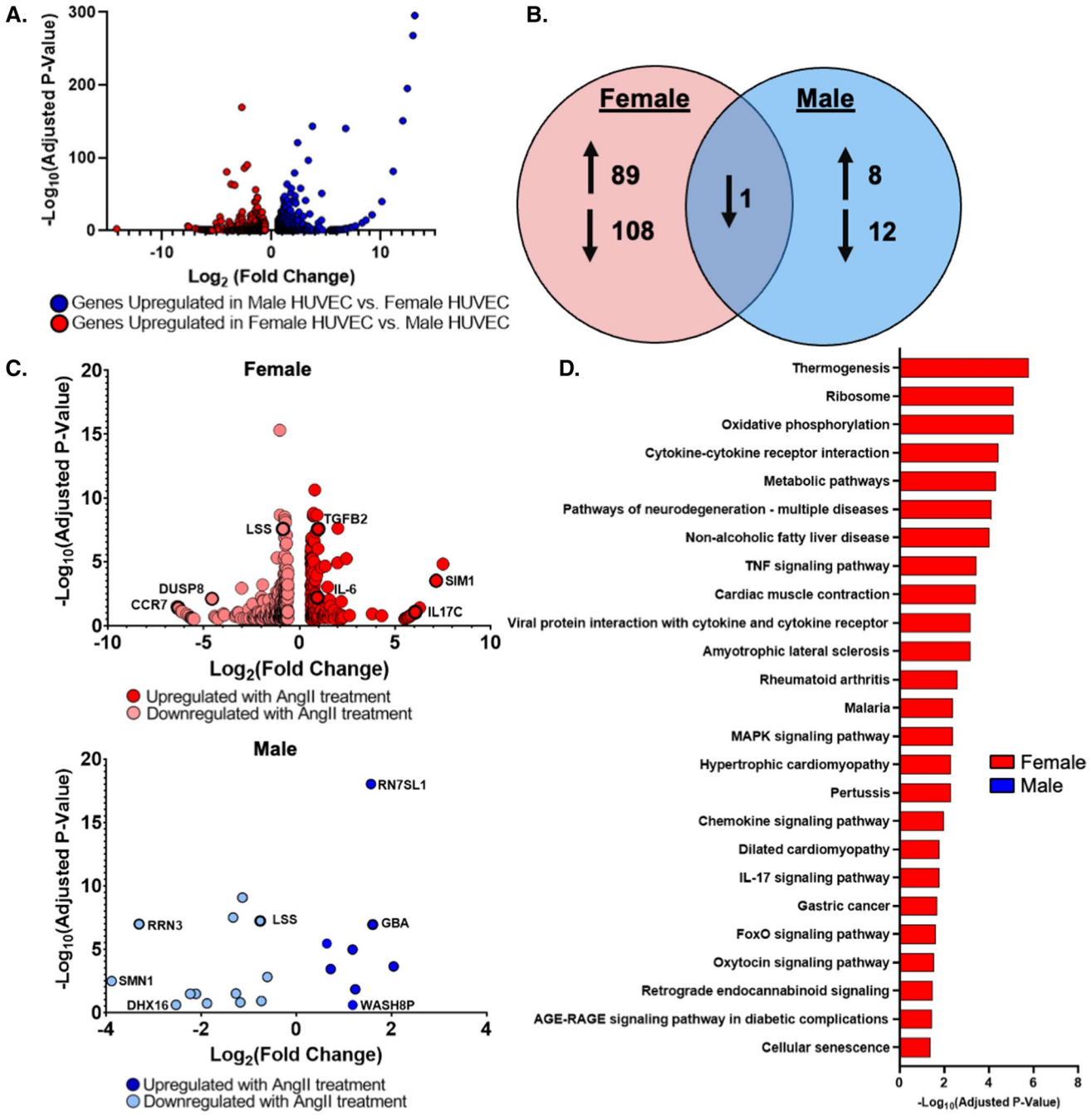

Fig. 1 Female EC differentially expressed more genes in response to AngII treatment. **A** Volcano plot of RNA sequencing data from untreated pooled female and male HUVEC. Blue indicates genes upregulated in male vs. female HUVEC (512 genes), and red indicates genes upregulated in female vs. male HUVEC (622 genes). Graph demonstrates data relative to male HUVEC where a positive Log_2FC indicates upregulation in male HUVEC and a negative Log_2FC indicates downregulation in male HUVEC relative to female. **B** Venn Diagram of gene expression changes in pooled female and male HUVEC treated with 1 μM AngII for 24 h. **C** Volcano plots of genes that were differentially expressed following 24 h of AngII treatment in female and male HUVEC. A full table of all differentially expressed genes is in the supplemental data, and gene names are defined in the glossary. **D** KEGG pathways significantly altered by AngII treatment containing more than three differentially expressed genes. Significant with $Log_2FC > 0.6$, and adjusted p-value < 0.3. n = 3 samples for each condition from pooled HUVEC in RNA sequencing data. Female and male HUVEC were pooled from three donors per sex

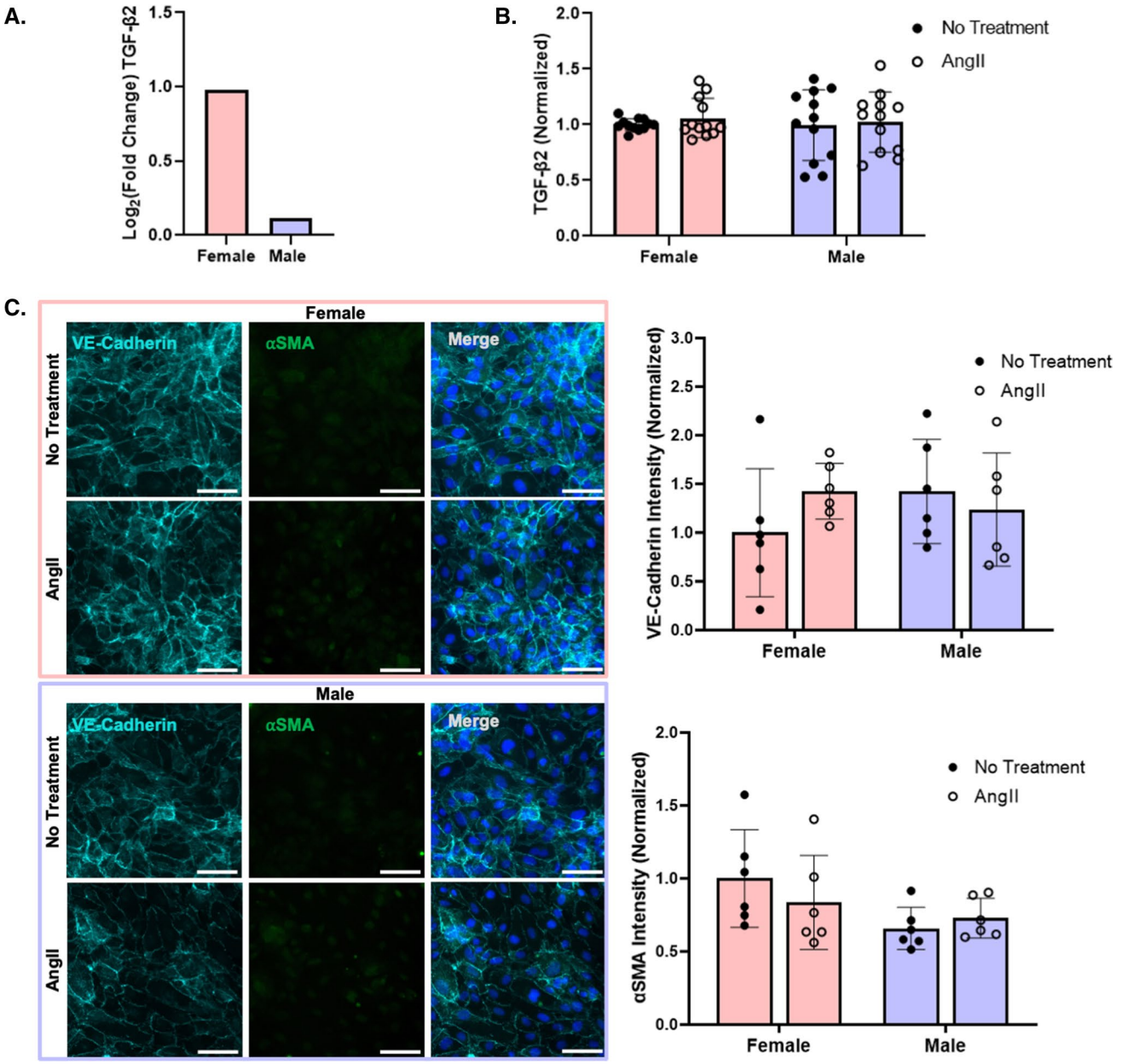

Fig. 2 AngII increased *TGFβ2* mRNA expression in female as compared to male HUVEC, but TGFβ2 protein and EndMT did not change with AngII or sex. **A** RNA-seq of changes in *TGFβ2* gene expression following 24 h of 1 μM AngII treatment in pooled male and female HUVEC (n = 3 samples per condition). **B** TGFβ2 protein after 24 h of 1 μM AngII treatment in pooled male and female HUVEC, as measured by ELISA (n = 12 samples; 3 pooled HUVEC samples per condition in each experiment, with the experiment repeated 4 times). **C** Representative fluorescent microscopy images of endothelial (VE-cadherin, light blue) and mesenchymal (αSMA, green) markers, with Hoescht-labeled nuclei (dark blue) in female and male HUVEC following 24 h of 1 μM AngII treatment, with quantification (n = 6 samples; 3 pooled HUVEC samples per condition in each experiment, with the experiment repeated 2 times). Scale = 50 μm. TGFβ2 protein and fluorescence intensity were normalized to untreated female cells

cytokine TNFα. In the presence of TNFα, AngII increased IL-6 protein release by 36% in pooled female but not male HUVEC (Fig. 3B, C). We then determined if the increased IL-6 release enhanced WBC adhesion using the male and female pooled HUVEC, individual donor HUVEC, and individual donor HPAEC. WBC adhesion was elevated by 33% in female, but not male, EC treated with AngII in the presence of TNFα (Fig. 3D–F; Supplemental Figs. 1, 2). These data suggest that AngII exposure in the presence of an additional inflammatory stimuli leads to a cooperative increase in inflammation response in female but not male endothelial cells.

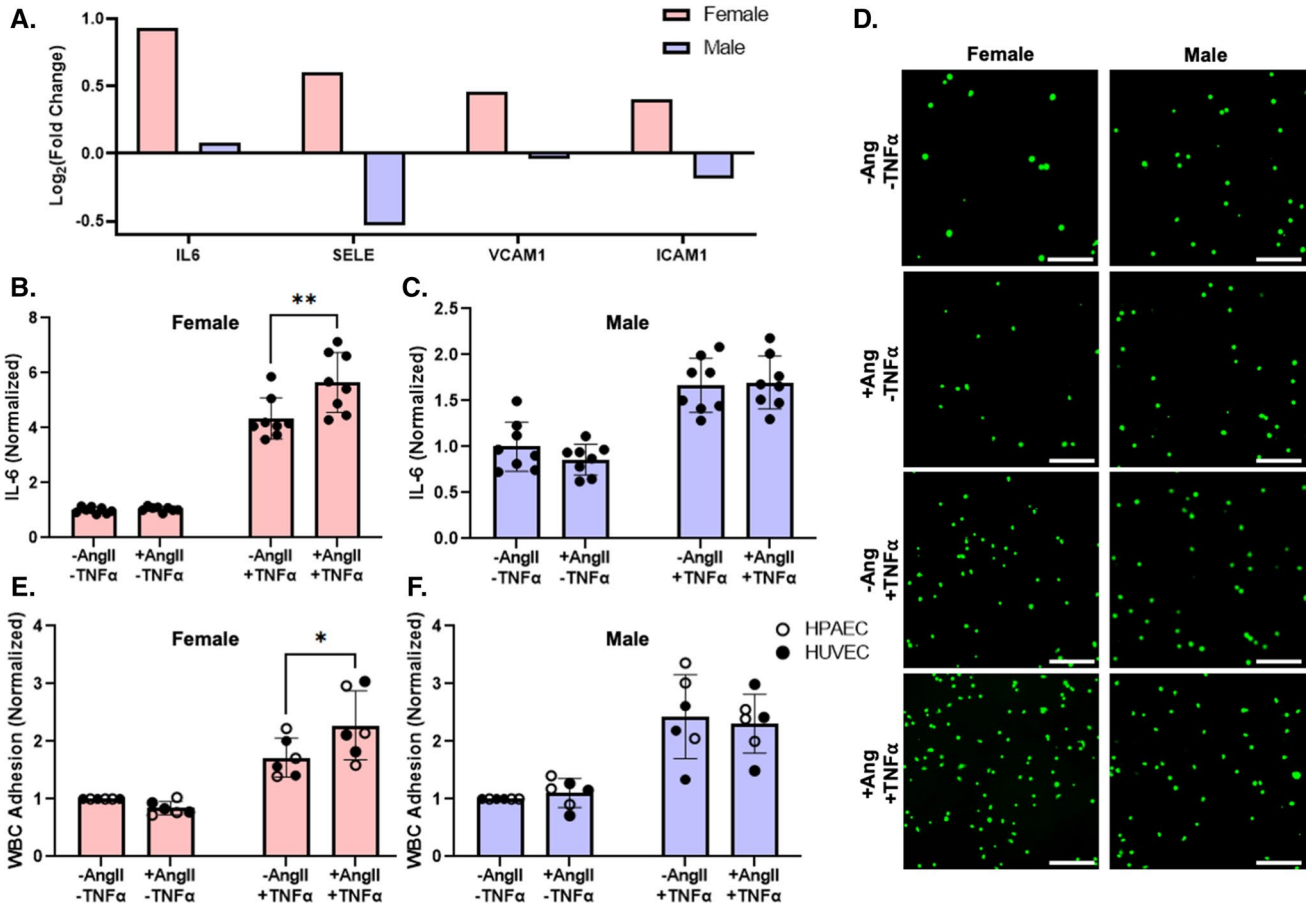

Fig. 3 Female EC had higher *IL-6* mRNA expression than male HUVEC following AngII treatment but required concurrent TNFα exposure to show higher IL-6 protein and WBC adhesion. **A** *IL-6, SELE, VCAM1, and ICAM1* gene expression from RNA sequencing in pooled female and male HUVEC following 24 h of 1 μM AngII treatment (n = 3 samples per condition). **B** Female and **C** male pooled HUVEC IL-6 protein release following 24-h treatment ± 1 μM AngII and ± 1 ng/mL TNFα, measured via ELISA (n = 8 samples; 4 samples per condition in each experiment, with the experiment repeated 2 times). **D** Representative WBC adhesion fluorescent microscopy images (calcein, green). **E** Female and **F** male pooled HUVEC, individual donor HUVEC, and individual donor HPAEC quantified WBC adhesion following 24-h treatment ± 1 μM AngII and ± 1 ng/mL TNFα (n = 6 donors per sex; each datapoint averaged from 3 samples per donor per condition). Scale = 100 μm. Data analyzed with two-way ANOVA. *p < 0.05, **p < 0.01. IL6 protein concentration and WBC adhesion normalized to untreated cells for each sex

Oxidative phosphorylation was identified as a significantly changed pathway via KEGG analysis. Indeed, nine genes involved in mitochondrial respiration were upregulated in female, but not male, pooled HUVEC following 24 h of AngII treatment (Fig. 4A). As ROS are a by-product of mitochondrial respiration, and AngII is known to increase endothelial ROS [27], we hypothesized that female EC treated with AngII would have higher ROS than male EC. Female and male pooled HUVEC, individual donor HUVEC, and individual donor HPAEC were treated with ± 1 μM AngII for 24 h and then incubated with Carboxy-H_2DCFDA, a general ROS indicator. Female HUVEC and HPAEC demonstrated a 33% increase in ROS following AngII treatment, while male HUVEC and HPAEC did not show an increase in ROS (Fig. 4B; Supplemental Fig. 3). However, individual donor female HCAEC did not increase ROS following AngII treatment (Supplemental Fig. 4).

We then evaluated if the increase in ROS was due to a rise in superoxide production as a byproduct of mitochondrial metabolism. When we labeled AngII-treated pooled female and male HUVEC with the mitochondrial ROS indicator MitoSOX, we observed that mitochondrial superoxide increased by 19% in the female but not male HUVEC (Fig. 5A). However, while pooled female HUVEC had 17% higher oxygen consumption rate (OCR; oxidative phosphorylation) and 17% higher mitochondrial ATP production than pooled male HUVEC by Seahorse dynamic metabolic measurements, neither OCR nor mitochondrial ATP changed with AngII treatment (Fig. 5B–D). Proton leak, defined as respiration that is not coupled to ATP production, was similar across all conditions (Fig. 5E). Although female HUVEC

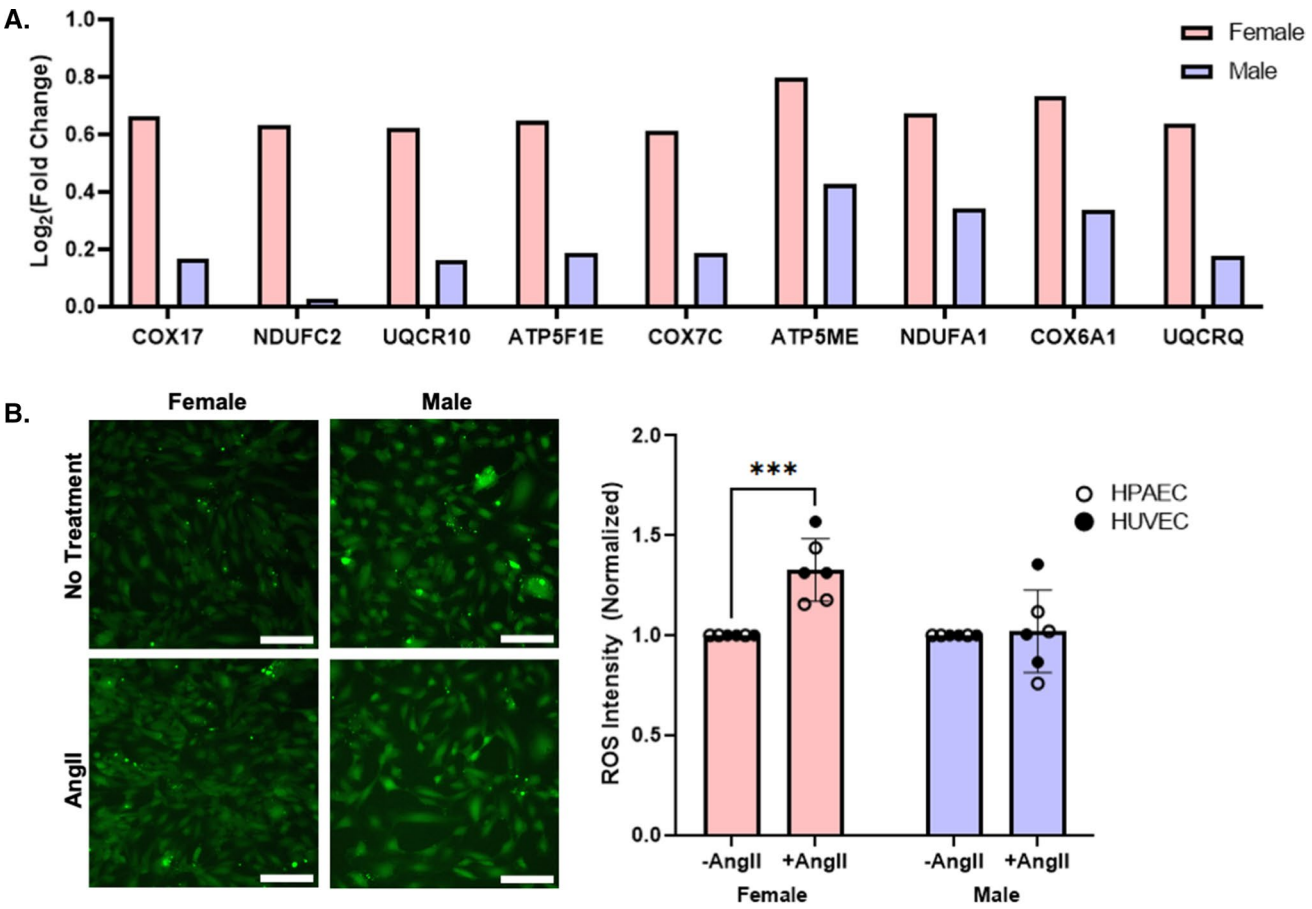

Fig. 4 Female EC increased ROS production in response to AngII compared to male EC. **A** RNA-seq of differentially expressed genes associated with mitochondrial respiration were elevated in pooled female but not male HUVEC following AngII treatment (n = 3 samples per condition). **B** Representative images and quantification of ROS production, measured via Carboxy-H_2DCFDA (green), in female versus male pooled HUVEC, individual donor HUVEC, and individual donor HPAEC following 24 h of AngII treatment (n = 6 donors per sex; each datapoint averaged from 3 samples per donor per condition)

had higher mitochondrial metabolism than male HUVEC, this did not appear to relate to the elevated ROS observed in AngII-treated female HUVEC.

We therefore examined an alternative pathway by which ROS production could be elevated in female HUVEC treated with AngII. *CYBB*, the gene for NOX2, escapes from X-chromosome inactivation [7]. NOX2 is the catalytic subunit of NADPH oxidase, which produces superoxide when activated and assembled in the cell membrane. RNA-sequencing showed *CYBB* gene expression to be higher in pooled female than male HUVEC, but due to high variability in the data, this was not statistically significant. We therefore repeated gene expression measurements by RT-qPCR and showed that *CYBB* gene expression was 4 times higher in pooled female compared to pooled male HUVEC and in female compared to male HPAEC from one donor (Fig. 6A). We then knocked down *CYBB* via siRNA in pooled HUVEC and confirmed significant NOX2 protein reduction after 24 h by Western blot (Fig. 6B). Using the more general, cell permeable ROS indicator Carboxy-H_2DCFDA, we again demonstrated elevated ROS in AngII-treated female but not male HUVEC. However, in HUVEC with NOX2 knocked down, AngII treatment failed to significantly elevate ROS in female or male cells (Fig. 6C, D).

Discussion

Elevated AngII is associated with many diseases, including PAH [24] and Alzheimer's disease [26], that are more likely to be diagnosed in women than men [2, 3]. Since EC have sexually dimorphic transcriptomes [5], we investigated how female and male EC respond differently to AngII. We now show that female EC have more extensive transcriptional changes in response to AngII as compared to male EC. While changes in *TGF-β2* gene expression did not lead to altered EC phenotype in vitro, we did observe elevated immune and oxidative stress responses to AngII in female

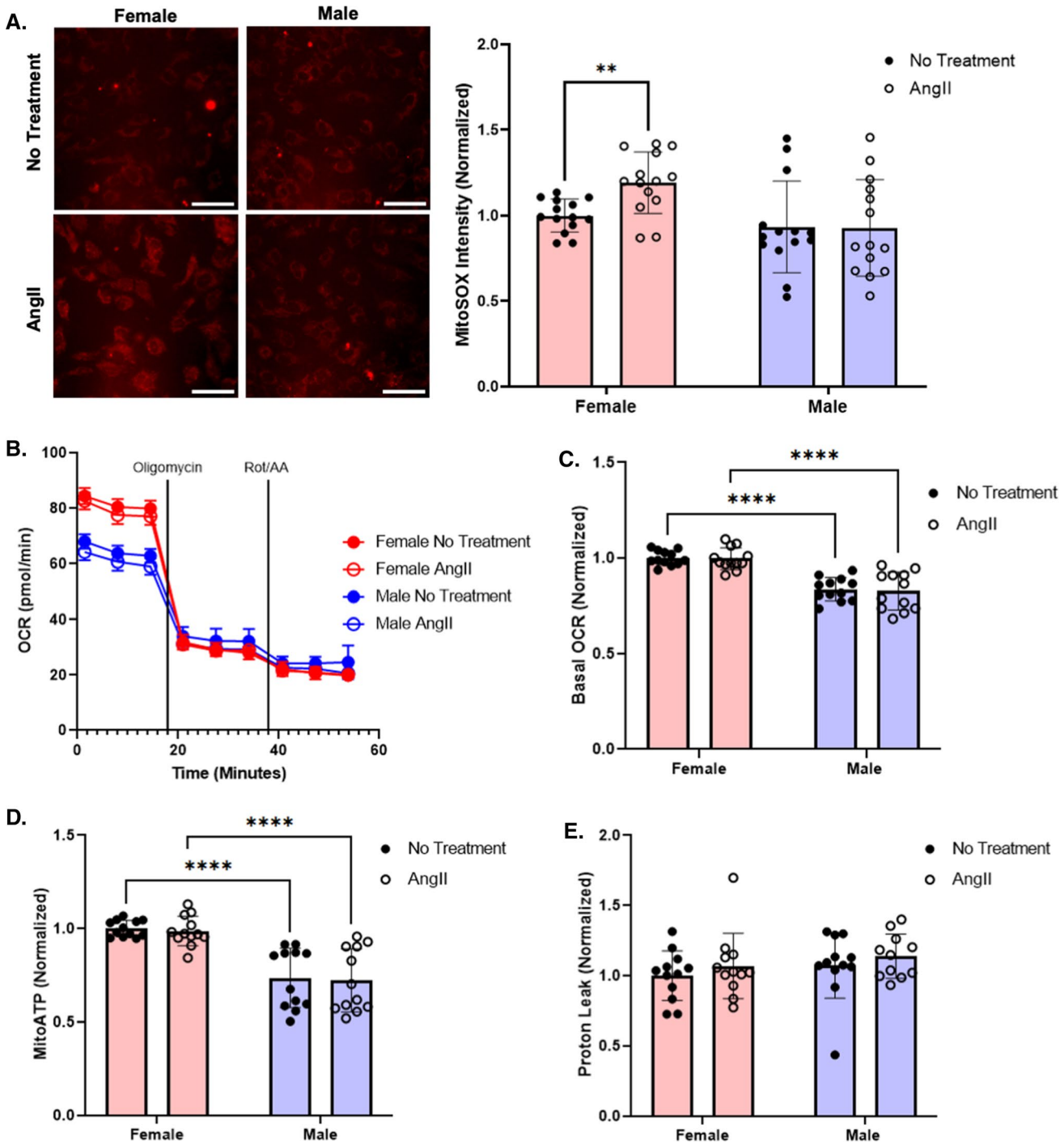

Fig. 5 Female EC increased superoxide in response to AngII compared to male HUVEC. **A** Mitochondrial superoxide production in pooled female versus male HUVEC following 24 h of AngII treatment measured via MitoSOX (red) (n = 14; 7 samples per condition in each experiment, with the experiment repeated 2 times). Scale = 100 µm. **C** OCR measured by Seahorse assay in pooled male and female HUVEC ± 1 µM AngII treatment (n = 12; 6 samples per condition in each experiment, with the experiment repeated 2 times). **D** Basal OCR, **E** mitochondrial ATP production, and **F** proton leak calculated from Seahorse OCR (n = 12; 6 samples per condition in each experiment, with the experiment repeated 2 times). MitoSOX and Seahorse data normalized to female untreated cells. Data analyzed with two-way ANOVA. *p < 0.05, **p < 0.01, ****p < 0.0001

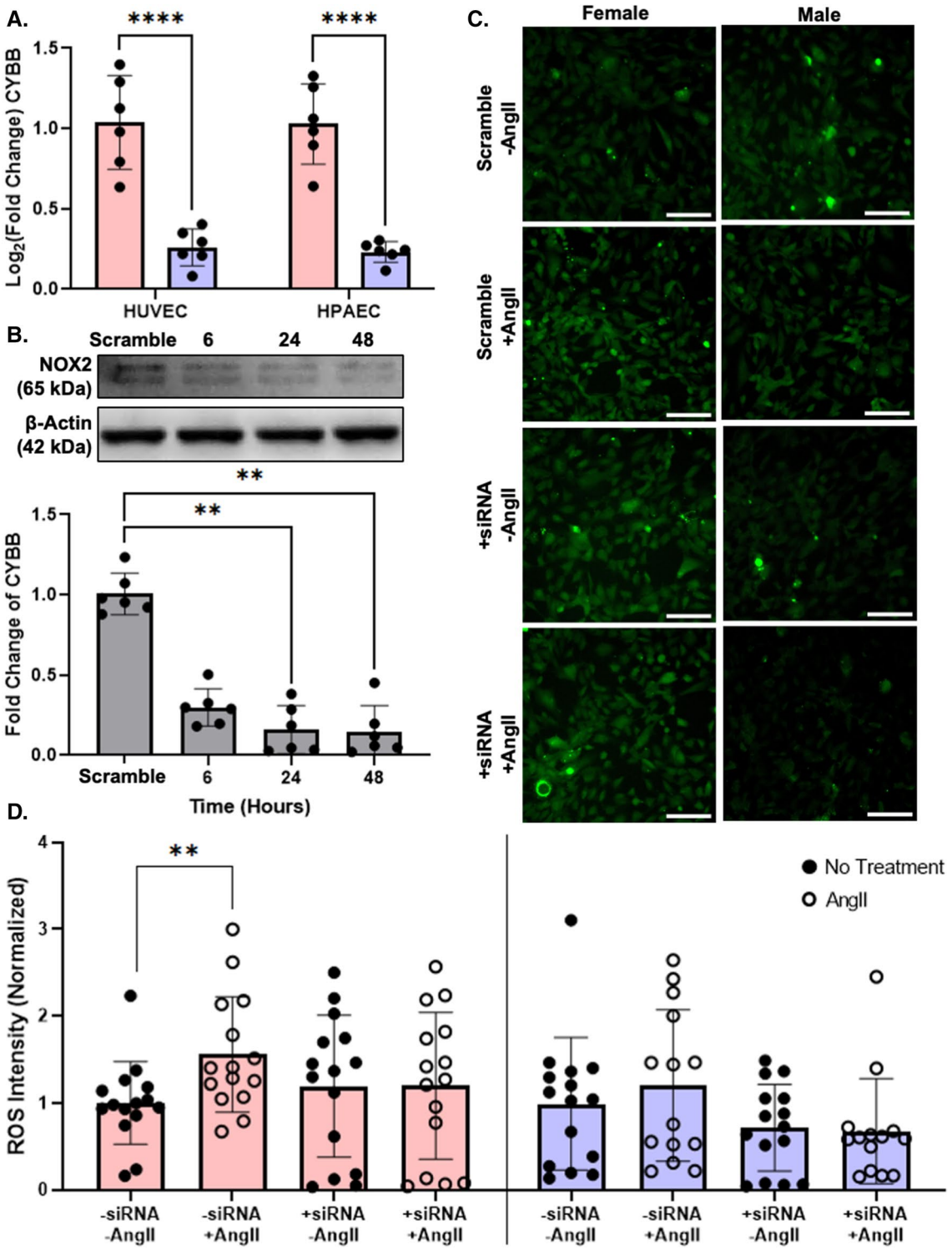

Fig. 6 *CYBB* was upregulated in female, but not male EC, which may contribute to elevated ROS production in AngII-treated female cells. **A** *CYBB* gene expression in untreated pooled female and male HUVEC and one female and male HPAEC donor by RT-PCR. Data analyzed with a Mann–Whitney test. **B** Western blot of NOX2 and β-Actin, with quantification, in pooled HUVEC treated with scramble siRNA or *CYBB* siRNA for 6–48 h. Data analyzed using Kruskal–Wallis test. **C** Representative fluorescent microscopy images of carboxy-H_2DCFDA (green) as an ROS indicator in pooled female and male HUVEC following *CYBB* siRNA (or scramble siRNA) and ± 1 μM AngII treatment for 24 h. Scale = 100 μm. **D** ROS quantification following siRNA knockdown. Data analyzed using two-way ANOVA with Tukey's correction for multiple comparisons *$p < 0.05$, **$p < 0.01$, ***$p < 0.001$, ****$p < 0.0001$. Western blot and ROS intensity were normalized to untreated female cells

EC as compared to male EC. Our study indicates that female EC have a stronger reaction to AngII, which may contribute to higher rates of AngII-related diseases in women.

Most studies of sex differences investigate specifically the impacts of sex hormone (estrogen and testosterone) exposure. However, hormone exposure is not the only differentiating factor between men and women. Phenotypic sex differences between men and women are a combination of the effects of sex chromosomes, genetic variation through copy number variants and single nucleotide polymorphisms, and epigenetic regulation by endogenous factors such as hormones or exogenous factors like environmental exposures [28]. Additionally, through the process of escape from XCI, genes on the second silenced X-chromosome in female cells can be reactivated, essentially doubling their gene expression. In this paper, we examine sex differences in response to AngII in neonatal umbilical vein endothelial cells, which were not exposed to sex hormones. We further validated our findings using adult pulmonary artery endothelial cells to demonstrate that sex differences were maintained regardless of cell age and hormone exposure.

Our RNA-sequencing data confirm prior studies that demonstrated gene expression changes in male and female HUVEC [5]. Indeed, sex differences have been observed in most tissues of the body [29]. A similar previous study reported 2,528 differentially expressed genes between male and female HUVEC in boy-girl twin pairs [5]; however, an adjusted p-value of < 0.1 was considered significant with no required Log_2FC cutoff, whereas we chose a more stringent cutoff of adjusted p-value < 0.3 and $Log_2FC > 0.6$. We now further show that female HUVEC have more differentially expressed genes compared to male HUVEC when treated with AngII. In male HUVEC, none of the differentially expressed genes were in the same KEGG pathway. Female HUVEC, on the other hand, had 25 KEGG pathways with 3 or more differentially expressed genes. Many of the differentially expressed genes were included in multiple KEGG pathways. For example, thermogenesis, oxidative phosphorylation, and metabolism KEGG pathways had almost entirely overlapping differential gene expression (electron transport chain, specifically cytochrome C reductase, cytochrome C oxidase, NADH dehydrogenase, and F-type ATPase). Seven out of eleven differentially expressed genes associated with the neurodegeneration KEGG pathway also overlapped with oxidative phosphorylation. These synergies suggest that differentially expressed genes in AngII-treated female cells could have wide-reaching cellular effects.

Although TGF-β2 production is known to increase EndMT [30], and female AngII-treated cells showed an increase in *TGF-β2* gene expression, we did not observe an increase in TGF-β2 released from the cells in male or female HUVEC treated with AngII. Generally, TGF-β2 is translated in the endoplasmic reticulum where it dimerizes and binds to latent TGF-β binding proteins (LTBP). The TGF-β2-LTBP complex is secreted, after which activating factors dissociate the complex. Active TGF-β2 then binds to TGF-β receptors on cells [31]. TGF-β2 can be secreted without LTBP [32], although LTBP promotes its folding and secretion [33]. We did not observe increased *LTBP* gene expression in female HUVEC, which could explain why TGF-β2 protein release was not increased in these cells following AngII treatment.

Furthermore, increased *TGF-β2* gene expression in female AngII-treated HUVEC did not induce EndMT, as measured by decreased endothelial markers and increased fibrotic markers. Maleszewska et al. proposed that elevated IL-1β is necessary for inducing EndMT, while TGF-β2 is essential to sustaining EndMT [34]. *IL-1β* was not differentially expressed in male or female HUVEC following AngII, which could mean that EndMT was not induced. Alternatively, other secondary stimuli such as TNF-α [35] and hydrogen peroxide [36] have been proposed to supplement TGF-β2-related EndMT. Sex differences in valvular interstitial cells were accentuated on soft and stiff hydrogels compared to tissue culture plastic [37], thus we might have observed functional changes in EndMT on softer substrates. Finally, *TGF-β2* gene expression may take longer to lead to cell functional changes [34–36, 38]. Although we did not observe cell function changes due to AngII-induced increased *TGF-β2* gene expression in female HUVEC, differences may occur with secondary stimuli, on softer substrates, or at longer times.

We similarly observed increased *IL-6* gene expression in AngII-treated HUVEC with no change in secreted protein or EC inflammatory response. *IL-6* mRNA is relatively unstable, with a 30-min half-life [39]. *IL-6* mRNA is stabilized by Arid5a [40], and its degradation is accelerated by Regnase-1 (*Zc3h12a)* [41]. Neither *ARID5A* nor *ZC3H12A* were differentially expressed in female EC following AngII treatment; therefore, *IL-6* mRNA may have been too unstable in AngII-treated cells to increase IL-6 protein secretion. TNF-α is an inflammatory stimulus that may increase *IL-6* mRNA stability [42], and in our cells, concurrent AngII and TNF-α treatment increased both IL-6 secretion and WBC adhesion in female HUVEC and HPAEC compared to TNF-α alone. WBC adhere to cell adhesion molecules on EC membranes including intercellular adhesion molecule-1 (ICAM-1), vascular cell adhesion protein-1 (VCAM-1), and E-Selectin. The E-selectin gene was significantly increased in female HUVEC following AngII treatment ($Log_2FC = 0.601$, $p < 0.0001$). Though *ICAM-1* ($Log_2FC = 0.399$) and *VCAM-1* ($Log_2FC = 0.455$) had statistically significant p-values, they did not reach our LogFC threshold for significance but may also be elevated in female HUVEC treated with AngII. Male HUVEC did not increase ICAM-1, VCAM-1, or E-Selectin expression following AngII treatment. Cell adhesion molecule gene upregulation likely contributes to increased WBC

adhesion to female, but not male, HUVEC following TNF-α and AngII treatment.

Finally, oxidative phosphorylation genes and ROS increased in female HUVEC treated with AngII, which correlated with elevated mitochondrial superoxide production. Seahorse ATP Rate Assays did not show a corresponding increase in mitochondrial respiration in either female or male HUVEC. Similar to increases in IL-6 following AngII treatment in female HUVEC, it may be that the cells are increasing gene expression of oxidative phosphorylation genes but require a second stimuli to actually increase OCR. We did find that *CYBB*, the gene encoding for NOX2, was overexpressed in female as compared to male cells and when knocked down, abrogated the AngII-induced increase in ROS in female HUVEC. *CYBB* was shown to escape X-chromosome inactivation [7], meaning it was expressed on both X chromosomes in female cells leading to double the gene expression. We similarly observed higher *CYBB* expression in female as compared to male HUVEC and HPAEC, indicating that *CYBB* may escape from X-chromosome inactivation in these cells. Interestingly, *CYBB* knockdown in female HUVEC did not reduce baseline ROS. Thus, NOX2 may be partially responsible for elevated ROS production in female HUVEC treated with AngII.

The HUVEC sex differences were partially replicated in EC from patients who were not neonates. Female HPAEC and HCAEC from donors aged 12–51 demonstrated elevated CYBB gene expression, congruent with our hypothesis that *CYBB* escapes X-chromosome inactivation. However, only female HPAEC had elevated ROS in response to AngII. This could relate to the specific vascular bed. HPAEC dysfunction is associated with PAH [43] and women are 2–4 times more likely to be diagnosed with PAH compared to men [2]. Indeed, differential gene expression associated with ROS production (including *CYBB*) has been proposed to be partially responsible for these sex differences [44]. Alternatively, age and sex hormone exposure may make sex differences in female EC less pronounced. In another study, ROS production was higher in female vs. male HUVEC at birth, but ROS production was higher in male vs. female human aortic endothelial cells in adults [5]. Additional studies are needed to determine how age and sex hormone exposure may impact female vs. male EC differences.

Conclusions

Cardiovascular disease manifests differently in women than men, and some of these differences may result from cellular transcriptomic differences due to genomic escape from XCI. Our data confirm that female HUVEC are transcriptomically distinct from male HUVEC. We further show that female EC had more extensive transcriptomic, inflammatory, and oxidative stress changes than male EC when exposed to the stress hormone AngII. These data suggest that transcriptomic differences between female and male EC may predispose women to certain cardiovascular diseases by altering the cellular response to a cardiovascular risk factor. Overall, our study supports the examination of sex differences at a cellular level to understand sexual dimorphisms in susceptibility to vascular diseases such as PAH and Alzheimer's disease.

Diversity Statement

Recent work in several fields of science has identified a bias in citation practices such that papers from women and other minority scholars are under-cited relative to the number of such papers in the field [45–53]. Here we sought to proactively consider choosing references that reflect the diversity of the field in thought, form of contribution, gender, race, ethnicity, and other factors. First, we obtained the predicted gender of the first and last author of each reference by using databases that store the probability of a first name being carried by a woman [49, 54]. By this measure (and excluding self-citations to the first and last authors of our current paper), our references contain 13.25% woman(first)/woman(last), 19.25% man/woman, 27.5% woman/man, and 40.0% man/man. This method is limited in that (a) names, pronouns, and social media profiles used to construct the databases may not, in every case, be indicative of gender identity and (b) it cannot account for intersex, non-binary, or transgender people. Second, we obtained predicted racial/ethnic category of the first and last author of each reference by databases that store the probability of a first and last name being carried by an author of color [55, 56]. By this measure (and excluding self-citations), our references contain 15.98% author of color (first)/author of color (last), 13.91% white author/author of color, 25.7% author of color/white author, and 44.42% white author/white author. This method is limited in that (a) names and Florida Voter Data to make the predictions may not be indicative of racial/ethnic identity, and (b) it cannot account for Indigenous and mixed-race authors, or those who may face differential biases due to the ambiguous racialization or ethnicization of their names. We look forward to future work that could help us to better understand how to support equitable practices in science.

Supplementary Information The online version contains supplementary material available at https://doi.org/10.1007/s12195-023-00762-2.

Author Contributions CMW and AMC conceived and designed the research. CMW, MNH, SMZ, and GS carried out the experiments. CMW, MNH, SMZ, NA, and DD analyzed data. CMW, MNH, SMZ, DFD, and AMC interpreted results of experiments. CMW and AMC prepared figures and drafted manuscript. CMW, MNH, SMZ, NA, DFD, and AMC edited, revised, and approved the final version of the manuscript.

Funding The authors gratefully acknowledge funding support from the National Institutes of Health (Grant Nos. R21EB028466 and R01HL140239-01) to AMC, the National Science Foundation (Grant Nos. CMMI 1916814 and CBET 1916997) to AMC, the Brain and Behavior Initiative at the University of Maryland through the BBI Seed Grant Program to AMC, NIMHD 5U54MD013376 subproject 8281 to DFD, the National Science Foundation Graduate Research Fellowship Program (Grant No. DGE 1840340) to CMW, NSF REU 1757745 to MNH, the University of Maryland ASPIRE program to SMZ, the University of Maryland Presidential Postdoctoral Fellowship to GSS, and the American Heart Association Postdoctoral Fellowship 916512 to GSS.

Data Availability All RNA sequencing data is publicly available under GSE211978.

Declarations

Conflict of interest Callie M. Weber, Mikayla N. Harris, Sophia M. Zic, Gurneet S. Sangha, Nicole S. Arnold, Douglas F. Dluzen, and Alisa Morss Clyne do not have any conflicts of interest, financial or otherwise, to declare.

Ethical Approval All procedures followed were in accordance with the ethical standards of the responsible committee on human experimentation (institutional and national) and with the Helsinki Declaration of 1975, as revised in 2000 (5). Informed consent was obtained from all patients being included in the study.

Animal Rights No animal studies were carried out by the authors for this article.

References

1. Hadi, H. A. R., C. S. Carr, and J. AlSuwaidi. Endothelial dysfunction: cardiovascular risk factors, therapy, and outcome. *Vasc. Health Risk Manag.* 1:183–198, 2005.
2. McGoon, M. D., R. L. Benza, P. Escribano-Subias, X. Jiang, D. P. Miller, A. J. Peacock, J. Pepke-Zaba, T. Pulido, S. Rich, S. Rosenkranz, S. Suissa, and M. Humbert. Pulmonary arterial hypertension: Epidemiology and registries. *J. Am. Coll. Cardiol.* 62:D51–D59, 2013.
3. Alzheimer's Association. Alzheimer's disease facts and figures. *Alzheimer's Dementia*. 15(3):321–387, 2022.
4. de Ritter, R., M. de Jong, R. C. Vos, C. J. H. van der Kallen, S. J. S. Sep, M. Woodward, C. D. A. Stehouwer, M. Lp, and S. A. E. Bots. Sex differences in the risk of vascular disease associated with diabetes. *Biol. Sex Differ.* 11:1–11, 2020.
5. Hartman, R. J. G., D. M. C. Kapteijn, S. Haitjema, M. N. Bekker, M. Mokry, G. Pasterkamp, M. Civelek, and H. M. den Ruijter. Intrinsic transcriptomic sex differences in human endothelial cells at birth and in adults are associated with coronary artery disease targets. *Sci. Rep.* 10:1–12, 2020.
6. Carrel, L., and H. F. Willard. X-inactivation profile reveals extensive variability in X-linked gene expression in females. *Nature*. 434:400–404, 2005.
7. Zhang, Y., A. Castillo-Morales, M. Jiang, Y. Zhu, L. Hu, A. O. Urrutia, X. Kong, and L. D. Hurst. Genes that escape X-inactivation in humans have high intraspecific variability in expression, are associated with mental impairment but are not slow evolving. *Mol. Biol. Evol.* 30:2588–2601, 2013.
8. Lorenz, M., J. Koschate, K. Kaufmann, C. Kreye, M. Mertens, W. M. Kuebler, G. Baumann, G. Gossing, A. Marki, A. Zakrzewicz, C. Miéville, A. Benn, D. Horbelt, P. R. Wratil, K. Stangl, and V. Stangl. Does cellular sex matter? Dimorphic transcriptional differences between female and male endothelial cells. *Atherosclerosis*. 240:61–72, 2015.
9. Lorenz, M., B. Blaschke, A. Benn, E. Hammer, E. Witt, J. Kirwan, R. Fritsche-Guenther, Y. Gloaguen, C. Bartsch, A. Vietzke, F. Kramer, K. Kappert, P. Brunner, H. G. Nguyen, H. Dreger, K. Stangl, P. Knaus, and V. Stangl. Sex-specific metabolic and functional differences in human umbilical vein endothelial cells from twin pairs. *Atherosclerosis*. 291:99–106, 2019.
10. Addis, R., I. Campesi, M. Fois, G. Capobianco, S. Dessole, G. Fenu, A. Montella, M. G. Cattaneo, L. M. Vicentini, and F. Franconi. Human umbilical endothelial cells (HUVECs) have a sex: Characterisation of the phenotype of male and female cells. *Biol. Sex Differ.* 5:1–12, 2014.
11. James, B. D., and J. B. Allen. Sex-specific response to combinations of shear stress and substrate stiffness by endothelial cells in vitro. *Adv. Healthc. Mater.* 10:2100735, 2021.
12. AbdAlla, S., A. el Hakim, A. Abdelbaset, Y. Elfaramawy, and U. Quitterer. Inhibition of ACE retards tau hyperphosphorylation and signs of neuronal degeneration in aged rats subjected to chronic mild stress. *Biomed. Res. Int.* 2015:917156, 2015.
13. Choi, H., T. L. Leto, L. Hunyady, K. J. Catt, S. B. Yun, and G. R. Sue. Mechanism of angiotensin II-induced superoxide production in cells reconstituted with angiotensin type 1 receptor and the components of NADPH oxidase. *J. Biol. Chem.* 283:255–267, 2008.
14. Romero, J. C., and J. F. Reckelhoff. Role of angiotensin and oxidative stress in essential hypertension. *Hypertension*. 34:943–949, 1999.
15. Bruner, C. A., J. M. Weaver, and G. D. Fink. Sodium-dependent hypertension produced by chronic central angiotensin II infusion. *Am. J. Physiol. Heart Circ. Physiol.* 18:H321, 1985.
16. Heeneman, S., J. F. M. Smits, P. J. A. Leenders, P. M. H. Schiffers, and M. J. A. P. Daemen. Effects of angiotensin II on cardiac function and peripheral vascular structure during compensated heart failure in the rat. *Arterioscler. Thromb. Vasc. Biol.* 17:1985–1994, 1997.
17. Landmesser, U., H. Cai, S. Dikalov, L. McCann, J. Hwang, H. Jo, S. M. Holland, and D. G. Harrison. Role of p47phox in vascular oxidative stress and hypertension caused by angiotensin II. *Hypertension*. 40:511–515, 2002.
18. Madhur, M. S., S. A. Funt, L. Li, A. Vinh, W. Chen, H. E. Lob, Y. Iwakura, Y. Blinder, A. Rahman, A. A. Quyyumi, and D. G. Harrison. Role of interleukin 17 in inflammation, atherosclerosis, and vascular function in apolipoprotein e-deficient mice. *Arterioscler. Thromb. Vasc. Biol.* 31:1565–1572, 2011.
19. Li, W. J., Y. Liu, J. J. Wang, Y. L. Zhang, S. Lai, Y. L. Xia, H. X. Wang, and H. H. Li. "angiotensin II memory" contributes to the development of hypertension and vascular injury via activation of NADPH oxidase. *Life Sci.* 149:18–24, 2016.
20. Ryan, M. J., S. P. Didion, S. Mathur, F. M. Faraci, and C. D. Sigmund. Angiotensin II-induced vascular dysfunction is mediated by the AT 1A receptor in mice. *Hypertension*. 43:1074–1079, 2004.
21. Rio, D. C., M. Ares, G. J. Hannon, and T. W. Nilsen. Purification of RNA using TRIzol (TRI Reagent). *Cold Spring Harb. Protoc.* 5:5439, 2010.
22. Tarca, A. L., S. Draghici, P. Khatri, S. S. Hassan, P. Mittal, J.-S. Kim, C. J. Kim, J. P. Kusanovic, and R. Romero. A novel signaling pathway impact analysis. *Bioinformatics*. 25:75–82, 2009.
23. Ahsan, S., and S. Drăghici. Identifying significantly impacted pathways and putative mechanisms with iPathwayGuide. *Curr. Protoc. Bioinform.* 2017:7.15.1-7.15.30, 2017.
24. de Man, F. S., L. Tu, M. L. Handoko, S. Rain, G. Ruiter, C. François, I. Schalij, P. Dorfmüller, G. Simonneau, E. Fadel, and F. Perros. Dysregulated renin–angiotensin–aldosterone system contributes to

pulmonary arterial hypertension. *Am. J. Respir. Crit. Care Med.* 186(8):780–789, 2012.
25. Ranchoux, B., F. Antigny, C. Rucker-Martin, A. Hautefort, C. Péchoux, H. J. Bogaard, P. Dorfmüller, S. Remy, F. Lecerf, S. Planté, S. Chat, E. Fadel, A. Houssaini, I. Anegon, S. Adnot, G. Simonneau, M. Humbert, S. Cohen-Kaminsky, and F. Perros. Endothelial-to-mesenchymal transition in pulmonary hypertension. *Circulation*. 131:1006–1018, 2015.
26. Kehoe, P. G., S. Miners, and S. Love. Angiotensins in Alzheimer's disease-friend or foe? *Trends Neurosci.* 32:619–628, 2009.
27. Birk, M., E. Baum, J. K. Zadeh, C. Manicam, N. Pfeiffer, A. Patzak, J. Helmstädter, S. Steven, M. Kuntic, A. Daiber, and A. Gericke. Angiotensin II induces oxidative stress and endothelial dysfunction in mouse ophthalmic arteries via involvement of AT1 receptors and NOX2. *Antioxidants*. 10:1238, 2021.
28. Khramtsova, E. A., L. K. Davis, and B. E. Stranger. The role of sex in the genomics of human complex traits. *Nat. Rev. Genet.* 20:494, 2019.
29. Oliva, M., et al. The impact of sex on gene expression across human tissues. *Science*. 369(eaba3066):2020, 1979.
30. Xiao, L., D. J. Kim, C. L. Davis, J. V. McCann, J. M. Dunleavey, A. K. Vanderlinden, N. Xu, S. G. Pattenden, S. V. Frye, X. Xu, and M. Onaitis. Tumor endothelial cells with distinct patterns of TGFβ-driven endothelial-to-mesenchymal transition endothelial-to-mesenchymal transition. *Cancer Res.* 75(7):1244–1254, 2015.
31. Robertson, I. B., and D. B. Rifkin. Regulation of the bioavailability of TGF-β and TGF-β-related proteins. *Cold Spring Harb. Perspect. Biol.*8:a021907, 2016.
32. Walton, K. L., Y. Makanji, J. Chen, M. C. Wilce, K. L. Chan, D. M. Robertson, and C. A. Harrison. Two distinct regions of latency-associated peptide coordinate stability of the latent transforming growth factor-β1 complex*. *J. Biol. Chem.* 285:17029–17037, 2010.
33. Miyazono, K., A. Olofsson, P. Colosetti, and C. H. Heldin. A role of the latent TGF-β1-binding protein in the assembly and secretion of TGF-β1. *EMBO J.* 10:1091–1101, 1991.
34. Maleszewska, M., J. R. A. J. Moonen, N. Huijkman, B. van de Sluis, G. Krenning, and M. C. Harmsen. IL-1β and TGFβ2 synergistically induce endothelial to mesenchymal transition in an NFκB-dependent manner. *Immunobiology*. 218:443–454, 2013.
35. Yoshimatsu, Y., I. Wakabayashi, S. Kimuro, N. Takahashi, K. Takahashi, M. Kobayashi, N. Maishi, K. A. Podyma-Inoue, K. Hida, K. Miyazono, and T. Watabe. TNF-α enhances TGF-β-induced endothelial-to-mesenchymal transition via TGF-β signal augmentation. *Cancer Sci.* 111:2385–2399, 2020.
36. Evrard, S. M., L. Lecce, K. C. Michelis, A. Nomura-Kitabayashi, G. Pandey, K. R. Purushothaman, V. D'Escamard, J. R. Li, L. Hadri, K. Fujitani, P. R. Moreno, L. Benard, P. Rimmele, A. Cohain, B. Mecham, G. J. Randolph, E. G. Nabel, R. Hajjar, V. Fuster, M. Boehm, and J. C. Kovacic. Endothelial to mesenchymal transition is common in atherosclerotic lesions and is associated with plaque instability. *Nat. Commun.* 7:11853, 2016.
37. Aguado, B. A., C. J. Walker, J. C. Grim, M. E. Schroeder, D. Batan, B. J. Vogt, A. G. Rodriguez, J. A. Schwisow, K. S. Moulton, R. M. Weiss, D. D. Heistad, L. A. Leinwand, and K. S. Anseth. Genes that escape X chromosome inactivation modulate sex differences in valve myofibroblasts. *Circulation*. 145:513–530, 2022.
38. Ma, J., G. van der Zon, M. A. F. V. Gonçalves, M. van Dinther, M. Thorikay, G. Sanchez-Duffhues, and P. ten Dijke. TGF-β-induced endothelial to mesenchymal transition is determined by a balance between SNAIL and ID factors. *Front. Cell Dev. Biol.* 9:182, 2021.
39. Paschoud, S., A. M. Dogar, C. Kuntz, B. Grisoni-Neupert, L. Richman, and L. C. Kühn. Destabilization of interleukin-6 mRNA requires a putative RNA stem-loop structure, an AU-rich element, and the RNA-binding protein AUF1. *Mol. Cell Biol.* 26:8228–8241, 2006.
40. Masuda, K., B. Ripley, R. Nishimura, T. Mino, O. Takeuchi, G. Shioi, H. Kiyonari, and T. Kishimoto. Arid5a controls IL-6 mRNA stability, which contributes to elevation of IL-6 level in vivo. *Proc. Natl. Acad. Sci. USA*. 110:9409–9414, 2013.
41. Matsushita, K., O. Takeuchi, D. M. Standley, Y. Kumagai, T. Kawagoe, T. Miyake, T. Satoh, H. Kato, T. Tsujimura, H. Nakamura, and S. Akira. Zc3h12a is an RNase essential for controlling immune responses by regulating mRNA decay. *Nature*. 458:1185–1190, 2009.
42. Elias, J. A., and V. Lentz. IL-1 and tumor necrosis factor synergistically stimulate fibroblast IL-6 production and stabilize IL-6 messenger RNA. *J. Immunol.* 145:161–166, 1990.
43. Simonneau, G., D. Montani, D. S. Celermajer, C. P. Denton, M. A. Gatzoulis, M. Krowka, P. G. Williams, and R. Souza. Haemodynamic definitions and updated clinical classification of pulmonary hypertension. *Eur. Respir. J.* 53:1801913, 2019.
44. Kostyunina, D. S., and P. McLoughlin. Sex dimorphism in pulmonary hypertension: the role of the sex chromosomes. *Antioxidants*. 10:779, 2021.
45. Mitchell, S. M., S. Lange, and H. Brus. Gendered citation patterns in international relations journals. *Int. Stud. Perspect.* 14:485–492, 2013.
46. Dion, M. L., J. L. Sumner, and S. M. Mitchell. Gendered citation patterns across political science and social science methodology fields. *Polit. Anal.* 26:312–327, 2018.
47. Caplar, N., S. Tacchella, and S. Birrer. Quantitative evaluation of gender bias in astronomical publications from citation counts. *Nat. Astron.* 1:141, 2017.
48. Maliniak, D., R. Powers, and B. F. Walter. The gender citation gap in international relations. *Int. Organ.* 67:889–922, 2013.
49. Dworkin, J. D., K. A. Linn, E. G. Teich, P. Zurn, R. T. Shinohara, and D. S. Bassett. The extent and drivers of gender imbalance in neuroscience reference lists. *bioRxiv*. 2020. https://doi.org/10.1101/2020.01.03.894378.
50. Bertolero, M. A., J. D. Dworkin, S. U. David, C. L. Lloreda, P. Srivastava, J. Stiso, D. Zhou, K. Dzirasa, D. A. Fair, A. N. Kaczkurkin, B. J. Marlin, D. Shohamy, L. Q. Uddin, P. Zurn, and D. S. Bassett. Racial and ethnic imbalance in neuroscience reference lists and intersections with gender. *bioRxiv*. 64:583, 2020.
51. Wang, X., J. D. Dworkin, D. Zhou, J. Stiso, E. B. Falk, D. S. Bassett, P. Zurn, and D. M. Lydon-Staley. Gendered citation practices in the field of communication. *Ann. Int. Commun. Assoc.* 2021. https://doi.org/10.1080/23808985.2021.1960180.
52. Chatterjee, P., and R. M. Werner. Gender disparity in citations in high-impact journal articles. *JAMA Netw. Open*.4:e2114509, 2021.
53. Fulvio, J. M., I. Akinnola, and B. R. Postle. Gender (im)balance in citation practices in cognitive neuroscience. *J. Cogn. Neurosci.* 33:3–7, 2021.
54. Zhou, D., E. J. Cornblath, J. Stiso, E. G. Teich, J. D. Dworkin, A. S. Blevins, and D. S. Bassett. Gender Diversity Statement and Code Notebook v1.0. 2020. https://doi.org/10.5281/zenodo.3672110
55. Ambekar, A., C. Ward, J. Mohammed, S. Male, and S. Skiena. Name-ethnicity classification from open sources. 2009.
56. Sood, G., and S. Laohaprapanon. Predicting race and ethnicity from the sequence of characters in a name. arXiv:1805.02109, 2018.

Publisher's Note Springer Nature remains neutral with regard to jurisdictional claims in published maps and institutional affiliations.

Springer Nature or its licensor (e.g. a society or other partner) holds exclusive rights to this article under a publishing agreement with the author(s) or other rightsholder(s); author self-archiving of the accepted manuscript version of this article is solely governed by the terms of such publishing agreement and applicable law.